Title
Holmium-YAG Laser ablation characteristics in calvarial lamellar and cortical bone: The role of water and tissue micro-architecture

Journal
Lasers in Medical Science, 10(3)

ISSN
0268-8921

Authors
Wong, Brian Jet-Fei
Sung, Vivian
Berns, Michael W
et al.

Publication Date
1995-09-01

DOI
10.1007/bf02133329

Lasers in Medical Science 1995, **10**:181–188

Holmium-YAG Laser Ablation Characteristics in Calvarial Lamellar and Cortical Bone: The Role of Water and Tissue Micro-architecture

BRIAN JET-FEI WONG[a,b], VIVIAN SUNG[a], MICHAEL W. BERNS[a], LARS O. SVAASAND[c], JOSEPH NEEV[a]

[a]*Beckman Laser Institute and Medical Clinic, University of California, Irvine, California 92715, USA*
[b]*Department of Otolaryngology-Head and Neck Surgery, University of California, Irvine, California, USA*
[c]*Institute of Physical Electronics, The Norwegian Institue of Technology, Trondheim, Norway*

Correspondence to B.J.F. Wong, Beckman Laser Institute, and Medical Clinic, University of California, 1002 Health Sciences Road East, Irvine, California 92715, USA

Paper received 10 October 1995

Abstract. The effect of tissue micro-architecture and water content on ablation rates in bone is examined. Precisely machined and prepared porcine calvarial lamellar and cortical bone were ablated with a Holmium-YAG laser ($\lambda = 2.1\,\mu m$). Lamellar and cortical bone differ substantially in their tissue micro-architecture. Both are porous hard tissues, which differ predominantly in size and distribution of pores within the bone matrix. These hard tissues were ablated under physiological (wet) and chemically dehydrated conditions. The ablation rates over the range of energy densities examined assumes many linear characteristics. Ablation rate (as a function of fluence) is considerably higher for dehydrated cortical bone ($4.7\,\mu m\ cm^2\ J^{-1}$) compared to fresh cortical bone ($1.49\,\mu m\ cm^2\ J^{-1}$). This trend is also observed in lamellar bone ($2.31\,\mu m\ cm^2\ J^{-1}$ for wet and $0.37\,\mu m\ cm^2\ J^{-1}$ for dry). Under both physiological and dehydrated conditions, cortical bone was ablated faster. Mechanisms accounting for these observations are discussed.

INTRODUCTION

Lasers have gained rapid acceptance in middle ear surgery since the successful performance of a stapedotomy using an Argon laser in 1980 (1). Since then CO_2 ($\lambda = 10.6\,\mu m$), Argon ($\lambda = 488$–514 nm) and KTP–Nd-YAG ($\lambda = 532$ nm) systems have gained wide usage in the treatment of middle ear disorders (2–4), particularly for otosclerosis (5–8). Otosclerosis is a unique disorder of bone resorption and remodelling affecting only the otic capsule of the temporal bone (9). In laser surgery of the skull base and temporal bone, the bone tissue can vary considerably from the very spongy and trabecular bone of the mastoid cavity to the extremely dense bone encountered in the otic capsule or diseased stapes footplate as in otosclerosis. In particular, studies which have examined the use of lasers for performing stapedotomy operations in animals or cadaveric human tissue have all overlooked the issue of bone density and architecture (8, 10–15).

While CO_2, Argon and KTP–Nd-YAG have been effective in creating holes in the stapes footplate (stapedotomy procedure), there are practical limitations. With visible wavelengths, the absorption in bone and water is small and ablation is accomplished with the aid of a pigmented absorber such as a drop of blood or ablated soft tissue placed over the site of interest. Continued ablation depends on formation of carbonized organic matter acting as an absorber of visible wavelengths (16). This suggests a strong dependence on pyrolysis as a means of tissue destruction. In contrast, CO_2 has excellent absorption in both water and collagen (a major constituent of bone), but commercial CO_2 lasers require bulky articulated delivery systems coupled to a microscope-based micromanipulator. Clinical practice has not kept pace with the development of new laser systems and wavelengths. This is particularly true with respect to near and mid infra-red and ultra-violet wavelengths.

0268–8921/95/030181+08 $12.00/0

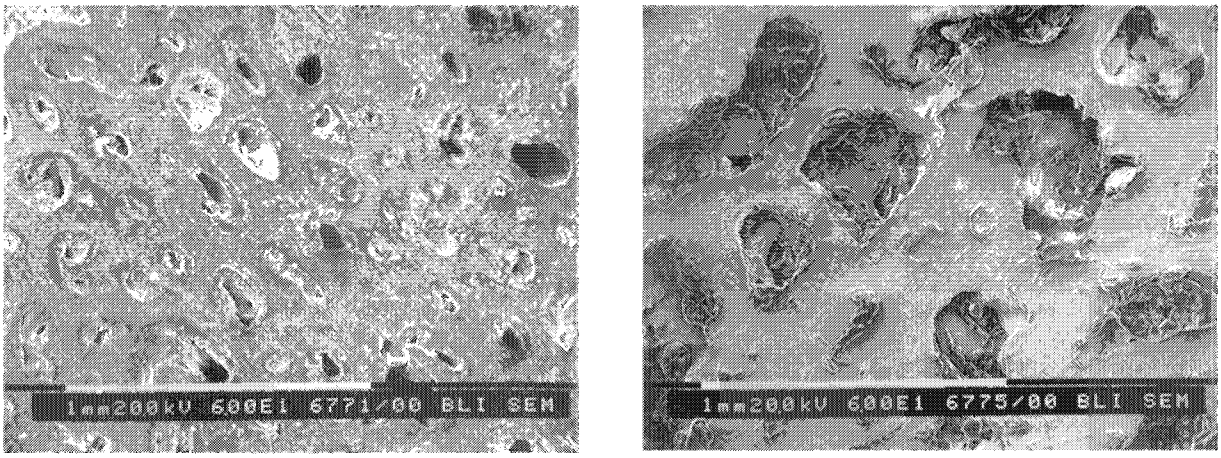

(a) (b)

Fig. 1. Scanning electron micrographs of prepared bone specimens (×75): (a) cortical bone—*substantia compacta* (fine pore structure); (b) lamellar bone—*substantia spongiosa* (coarse pore structure).

The Holmium-YAG (Ho-YAG) laser has been proposed for use in otolaryngologic surgical procedures (17) and has demonstrated utility in animal models for stapedotomy (12, 14), laryngeal surgery (18) and sinus surgery (19). Clinical applications in otolaryngology have included the use of the Ho-YAG laser to debulk extensive nasopharyngeal carcinoma (20) and for sinus surgery. In orthopaedics, Ho-YAG is used extensively for arthroscopic surgery (21). In orthopaedic surgery, the photoacoustic effects (popping sounds) and plasma plumes are more readily tolerated as most bone and joints are not surrounded by critical neurological structures in contrast to the ear which is essentially adjacent to the brain. The Ho-YAG laser produces little carbonization and coagulative necrosis and has drawn comparisons to CO_2, albeit with the advantage of fibre optic delivery. While the absorption coefficient for Erbium-YAG lasers in water is much higher ($\alpha = 13\,000\ cm^{-1}$) than Ho-YAG ($\alpha = 40\ cm^{-1}$), silica fibre optic cables are readily available in contrast to Erbium-YAG based systems.

While several authors have described the ablation process in bone using infra-red wavelengths (22–27), the role of water in this process and the influence of tissue architecture have not been completely addressed. Although Nuss et al measured ablation rates with Erbium-YAG lasers in dried guinea-pig calvarial bone, a comparison with fresh (hydrated) bone was not performed (24). Most studies on bone ablation have focused on long bones with an emphasis on orthopaedic applications (22, 23, 27). Long bones are composed of dense cortical bone surrounding an inner core of marrow-bearing highly cellular trabecular bone tissue with macroscopically visible pockets of soft tissue and fluid. The bones of the calvarial vault do not share this organization. First, calvarial bone does not contain marrow and varies in that it is composed of two layers of cortical bone tissue sandwiching an inner layer of lamellar tissue. The change from cortical to lamellar bone occurs gradually. As illustrated in the low power scanning electron microscopy photographs, in Fig. 1(a) the porous nature of cortical bone differs substantially from lamellar Fig. 1(b). While calvarial bone has been used to study ablation characteristics (24–26, 28), there are no studies which address these changes in tissue micro-architecture.

In the skull base and temporal bone, each clinical problem for which a laser may have potential application usually has a different type of bone tissue associated with it. One critical interaction is the influence of bone micro-architecture on the ablation process. In ear surgery, the bone encountered varies from being very compact as in cortical bone or otic capsule to very spongy such as in the mastoid cavity. This study used porcine cortical (substantia compacta) and lamellar bone (substantia spongiosa) as a model tissue for investigating laser–tissue interactions in bone tissue where the underlying tissue micro-architecture is variable. In addition, the role of water in the ablation process is examined. This is illustrated by demonstrating the ablation characteristics of a Ho-YAG laser on fresh and dehydrated specimens in these two bone tissues. The ablation rates for compact cortical

bone is compared to that of less compact lamellar bone. The role of pulse repetition rate and power density are described in dry lamellar bone. The influence of the tissue micro-architecture is discussed.

MATERIALS AND METHODS

A pulsed Ho-YAG laser in a free running mode ($\lambda = 2.1\,\mu m$, pulse width $250\,\mu s$ FWHM) was used to perform all ablation studies (Schwartz Electro-Optics Laser 1-2-3, Orlando, Florida, USA). Pulse repetition rate was varied from 2 to 7 Hz while energy delivered per pulse was varied between 30 and 130 mJ. The beam was focused with a standard CaF_2 lens with a focal length of 200 mm. Spot size was determined using thermal paper and maintained at 1 mm^2. Bone specimens were held in place with a caliper mounted on a x-y-z adjustable support. Energy output from the laser was monitored and determined before each ablation with a joulemeter (Gentec Model ED-500, Canada). Ablation rates (microns per pulse) were determined by measuring the time required for penetration of the bone specimen with a predetermined thickness. Completion of ablation was determined by placing a power meter behind the disc being studied. When the laser penetrates through the entire tissue specimen, the joulemeter is triggered. The meter activation energy is 1 mJ.

The specific methods for tissue preparation and machining have been previously described (29). Cortical and lamellar bone were harvested from the parietal and frontal bones of freshly sacrificed domestic pigs (Farmer John's Clougherty Packing Company, Vernon, California, USA). Soft tissues and periosteum were gently removed from the outer calvarial surface. An industrial plug cutter (Irwin Co, Model 43904, Wilmington, Ohio, USA) was used to obtain 0·5″ cylindrical cores of bone tissue that included both internal and external cortical surfaces. A low speed microstructural saw with a diamond wafering blade (Buehler, Model 11-1180 Isomet, Lake Bluff, Illinois, USA) machined the cylinder of bone into thin discs of uniform thickness varying from 0.85 to 0.95 mm. Care was taken to precisely machine cortical bone from the outer table of the cylindrical bone plug in order to obtain a specimen of as uniform density as possible. For lamellar bone, the cylinder was machined in its midsection to ensure that no cortical bone remnants were included with these specimens. No tissue was harvested from the cortical surface that abutted the dura mater.

For fresh tissue studies, the discs were placed in a cold saline bath at 4 °C. They were used within 24 h and allowed to equilibrate with ambient temperature in a 25 °C saline bath. For dry tissue investigations, the tissue was first fixed in formaldehyde for 24 h, then serially dehydrated with graded alcohol solutions. The tissue was preserved in formaldehyde to ensure safe storage and handling. Each individual disc was inspected for uniformity in thickness using a micrometer and evaluated visually with a low power microscope to ensure gross uniformity. Specimens with marked heterogeneity (e.g. suture lines, cracks) were discarded. Following completion of ablation, all fresh tissue was fixed in formaldehyde and serially dehydrated as described above.

Density of the cortical and lamellar bone tissue was determined by measuring the thickness and diameter of each individual disc weighing each specimen under dry conditions. Low power light micrographic observations were performed on several specimens to illustrate the variation in tissue architecture. The spatial density of pores per low power field was determined as well as the surface area of each pore via optical micrometry at × 64 magnification.

RESULTS

Density determinations and micrographic observations

The average densities were 0.98 mg mm^{-3} and 1.18 mg mm^{-3}, respectively, for cortical and lamellar bone. The standard deviations were 0.151 mg mm^{-3} and 0.146 mg mm^{-3}, respectively. There is significant overlap between these two populations. The strong similarity between the two tissues would suggest that the differences in ablation rate are not due to differences in mass per unit volume. Micro-architecture in lamellar and cortical bone specimens were assessed using low power light microscopy. Several observations are readily apparent. The two tissues share an overall similarity in terms of their architecture. As illustrated in Fig. 1, the structure of both these two tissues is honeycombed and trabecular in nature. However, they differ markedly in the size of the spaces within the bone matrix. In

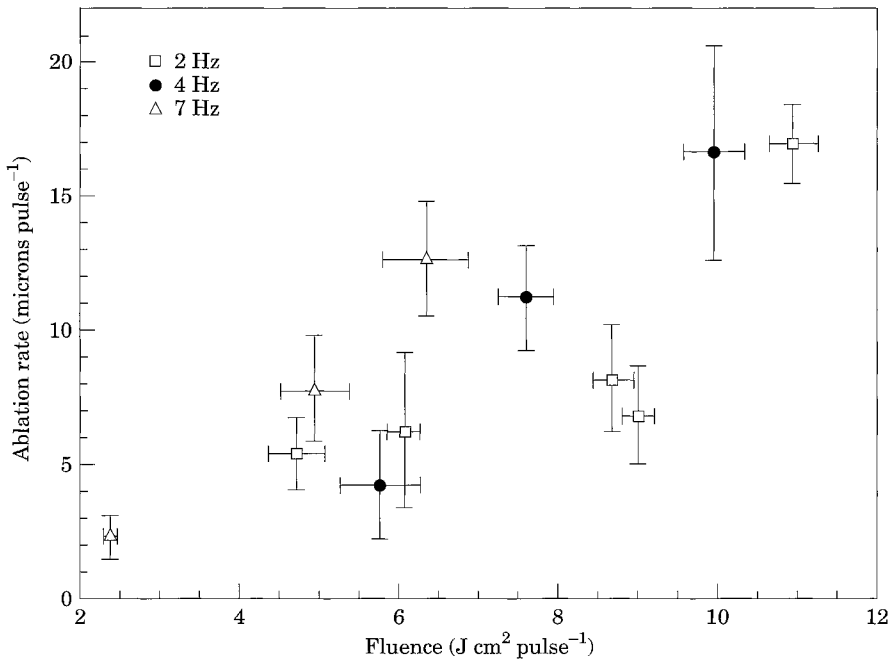

Fig. 2. Ablation rates as a function of pulse repetition rate in dehydrated lamellar bone.

living tissue, these regions (devoid of bone matrix) are filled with interstitial fluid and soft cellular elements such as blood or marrow components. The trabecular structure of the bone provides structural support while minimizing mass. The smaller resolution of the cortical bone architecture yields bone which is hard with respect to direct impacts. The coarser (or larger) lamellar bone allows for distribution of force. The average pore size was estimated to be 0.030 mm^2 ($\pm$ 0.023 mm^2 s.d.) for cortical bone and 0.26 mm^2 ($\pm$ 0.17 mm^2 s.d.) for lamellar bone. As a relative measure, the average number of pores per microscopic field ($\times$ 64) was 177.4 ($\pm$ 22.2 s.d.) and 38.8 ($\pm$ 6.9 s.d.) for cortical and lamellar bone, respectively.

Ablation rate as a function of pulse repetition rate

The ablation rate as a function of pulse repetition rate was determined in dehydrated lamellar bone. The depth of the hole created per laser pulse was determined for pulse energies varying from 2 J cm^{-2} up to 12 J cm^{-2} per pulse. Pulse repetition rate varied from 2 to 7 Hz and the results are depicted in Fig. 2. Linear regression analysis revealed correlation coefficients of 0.69, 0.89 and 0.90 for 2, 4 and 7 Hz, respectively. The rates of change of ablation efficiency with fluence were 2.0, 2.31 and 2.56 μm cm^2 J^{-1} for 2, 4 and 7 Hz, respectively. The results indicate a very linear dependence of ablation efficiency changes on energy per pulse. Increasing the pulse repetition rate results in a moderate change of this parameter.

Ablation rate as a function of pulse repetition rate with constant energy per pulse

With the energy per pulse kept constant at 5.30 J cm^{-2} per pulse $\pm$ 0.40 J cm^{-2}, the ablation rate as a function of pulse repetition rate was determined in dehydrated lamellar bone (Fig. 3). As frequency increases from 2 to 5 Hz, the ablation rate in terms of microns per second increases. High fluences for pulse repetition rates of 5 Hz could not be attained with the laser employed for these studies.

Ablation rate as a function of pulse repetition rate with constant power

When the power was kept constant at 17.6 W cm^{-2} $\pm$ 1.07 W cm^{-2}, and the ablation rate was determined in dry lamellar bone with the pulse repetition rate varied from 2 to 7 Hz, then the ablation rate in terms of microns per second was relatively constant (Fig. 4). The energy per pulse decreases with increasing pulse repetition rate.

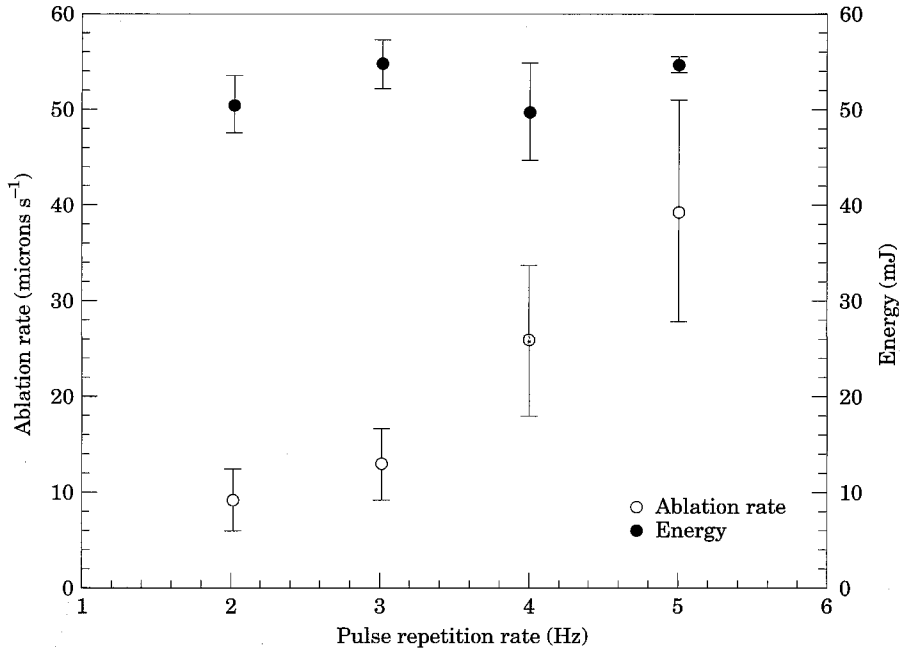

Fig. 3. Ablation rate as a function of pulse repetition rate with constant energy per pulse (5.3 J cm^{-2}). The ablation rate is in terms of microns per second.

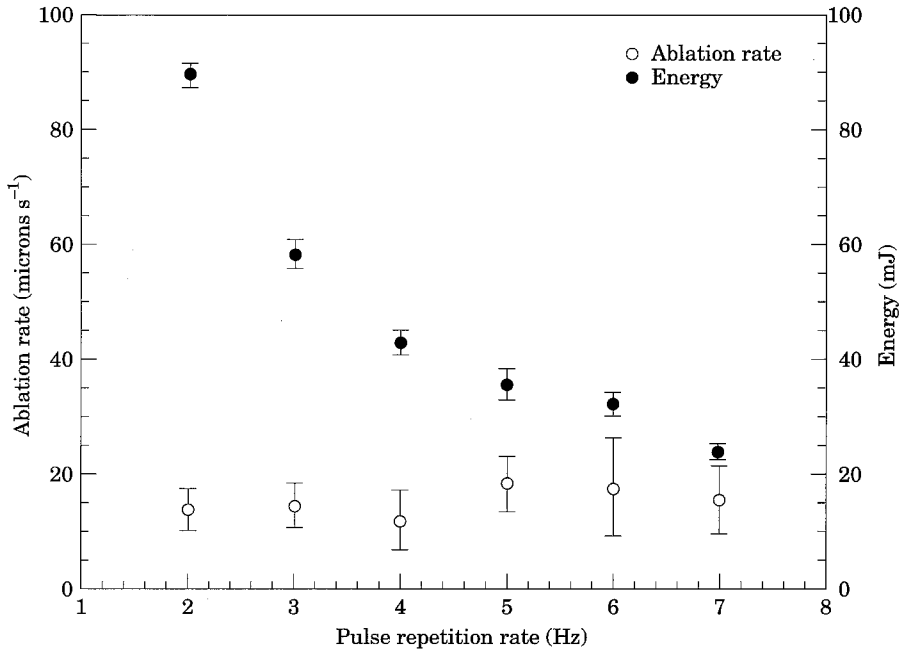

Fig. 4. Ablation rate as a function of pulse repetition rate with constant power (17 W cm^{-2}). Energy per pulse (J cm^{-2}) is plotted against pulse repetition rate. The ablation rate is in terms of microns per second.

Comparison of ablation rates between fresh and dehydrated lamellar and cortical bone

Fresh and dehydrated lamellar and cortical bones were ablated at pulse repetition rate of 4 Hz with energy per pulse varying from 2 J cm^{-2} up to 12 J cm^{-2}. The data is depicted in scatter diagrams with their corresponding regression lines as illustrated in Fig. 5. In all cases there appears to be a linear increase in ablation rates with pulse fluence. The weakest dependence is observed with fresh lamellar tissue as shown by the linear curve. Unfortunately, the correlation coefficient in this case is poor (r=0.52) despite the large number of data points. The slope of this curve is 0.37 μm

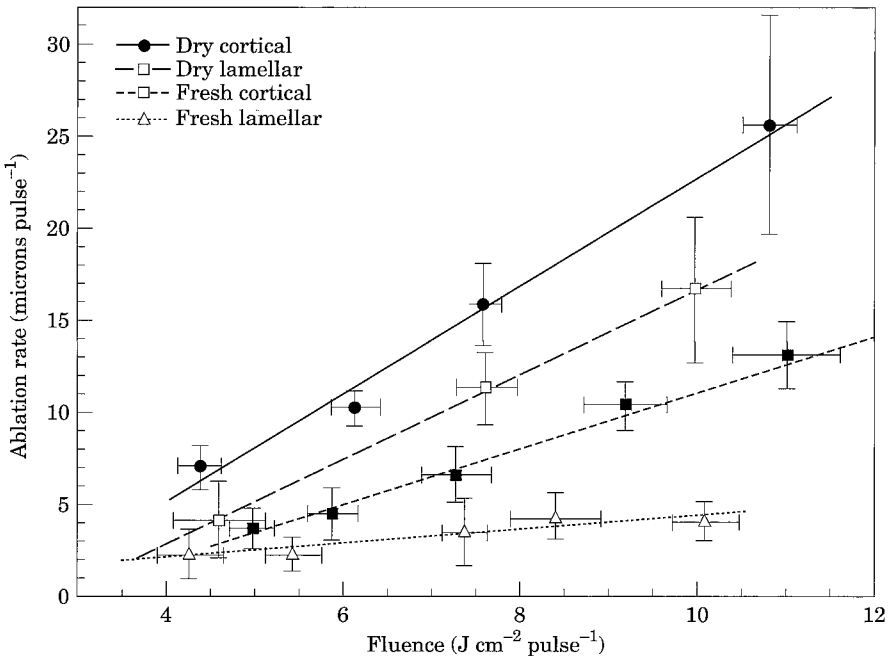

Fig. 5. Ablation rates for cortical and lamellar bone under physiological (wet) and dehydrated conditions.

$cm^2\ J^{-1}$ which is six times lower than the slope of the curve in dehydrated lamellar bone ($2.31\,\mu m\ cm^2\ J^{-1}$, $r=0.89$). The slope for dehydrated cortical bone is $4.70\,\mu m\ cm^2\ J^{-1}$ which is twice that of dried lamellar bone ($2.31\,\mu m\ cm^2\ J^{-1}$). With dehydrated cortical bone, excellent correlation ($r=0.93$) was noted. Fresh cortical bone demonstrated an ablation rate curve slope of $1.49\,\mu m\ cm^2\ J^{-1}$ with excellent correlation ($r=0.89$).

DISCUSSION

In this study, the ablation characteristics of wet (physiological) and dried calvarial lamellar and cortical porcine bone were described. The compact cortical bone (substantia compacta) differs from lamellar bone (substantia spongiosa) in terms of the intrinsic architecture of the bone itself. Both tissues share common features in that they are honeycombed structures with pockets filled with fluid or soft tissue that are surrounded by extremely dense bone matrix, which is approximately 35% collagen, 60% calcium phosphate (hydroxyapatite) and 5% water. In lamellar bone, the pockets are large and overall provide structural support to the calvarial vault while minimizing weight. Cortical bone must absorb the incident impact of blunt trauma and has smaller pockets interspersed in the bone matrix. In vivo, there is a gradation in this architecture as one moves from the cortical surfaces to the deeper lamellar bone tissue. In this study, only the outermost portion of the cortex and inner central region of the lamellar tissue were examined in order to emphasize the difference in structure. Although at this time, the authors do not have a complete theory of the effect of pore size on the ablation rate, this parameter could play an important role in the mechanical transients and thermal diffusion characteristics. Their quantification and correlation to ablation rates would be likely to help in further interpretation of the authors' data.

Some basic ablation characteristics of dehydrated lamellar bone were examined. Increasing pulse repetition rate from 2 to 4 Hz with constant energy delivery per pulse demonstrated minimal change in the ablation rate slope ($\mu m\ cm^2\ J^{-1}$) (Fig. 3). This implies that pulse-to-pulse residual effects, such as ablated debris, heat or density changes, were not significant enough to modify ablation characteristics. This purely additive effect in ablation is demonstrated between 2 and 4 Hz pulse repetition rate. At 5 Hz pulse repetition rate, the ablation rate slope ($\mu m\ cm^2\ J^{-1}$) increases slightly with the increase in frequency. This means that sandwiched between 0.25 s and 0.5 s pulse separation interval, these pulse-to-pulse effects are not significant enough to modify the ablation rate. Higher pulse repetition rates with constant energy per pulse produce successively larger ablation rates.

In the present system, the energy per pulse decreases inversely with respect to increasing pulse repetition rate such that when the power delivered is constant, then ablation rate per unit time is relatively constant though the ablation rate per pulse decreases (Fig. 4). The authors state this observation to the extent that this is a common phenomena with other Ho-YAG systems; it is important to keep this in mind.

In fresh lamellar bone, the ablation rate was determined at a pulse repetition rate of 4 Hz. The data depicted in Fig. 5 demonstrates increasing ablation rate with increasing energy per pulse, but the correlation is poor ($r=0.52$). In contrast to fresh lamellar bone, fresh cortical bone ablation at 4 Hz proceeds in a linear fashion with good correlation ($r=0.89$) (Fig. 5). The structural architecture of these tissues is similar, but differs in one important way. First, cortical bone contains many pockets; the size of the pockets is substantially smaller than the pockets in lamellar bone. These smaller pockets of water clearly require less energy to vaporize than their lamellar counterparts, and thus may explain the difference in ablation rates.

When dehydrated, cortical bone is ablated with good correlation ($r=0.93$) with an ablation rate of 4.71 μm cm^2 J^{-1} (Fig. 5). This rate is greater than that observed in lamellar bone. This difference in ablation between fresh (wet) cortical bone and dry cortical bone is significant. The effect of water in the ablation process is most dramatically illustrated in this tissue. The role of tissue architecture is exemplified by the differences in the ablation rates between fresh cortical and lamellar tissue.

The data appears to raise two questions that should be addressed. First, why do tissues with a smaller pocket/pore size (cortical bone) ablate quicker than those with larger pockets? Second, why do hydrated tissues ablate at a lower rate than their dry counterparts? In examining the effects of water on the ablation process, it should be noted that, in this study, dehydration referred to the removal of all water that filled the macroscopic pockets and pores of the tissue specimen. The most simple explanation for the decrease in ablation rate observed in wet tissues is that wet tissues have greater mass per unit volume than their dry counterparts and hence require more energy to ablate. The macroscopic pockets of water absorb part of the incident laser energy and must be vaporized for the ablation process to continue. The pockets are of variable size depending on the specific bone tissue. These pools of water may measure up to 0.25 mm^2 in area in lamellar bone in contrast with 0.03 mm^2 in cortical tissue. If ablation occurs via the production of vaporized water within the bone matrix (as opposed to the large pockets of water), then water should enhance ablation. This was not observed with these porous structures.

The density and type of bone used in these studies simulate those encountered in head and neck surgery. The ablation rates in hard tissues of differing microstructure were determined under both native and dehydrated conditions. Dehydrated porous bone tissues ablate more readily than their dry counterparts and this varies with the tissue micro-architecture. The ablation rate of bone with a fine pore structure (cortical) is greater than that with a coarser architecture (lamellar). As pulsed infra-red lasers find clinical application in ablating bone, tissue micro-architecture and water content status need to be considered in order to optimize treatment and better determine specific laser parameters.

ACKNOWLEDGEMENTS

The authors wish to thank Bill Walker of the Clougherty Packing Company for his assistance with tissue specimens, and Eric Cheung, Ann Hamilton, Glen Profeta and Jeff Andrews for their technical expertise. The authors would also like to thank Mark R. Dickinson PhD, George T. Hashisaki MD and Karen J. Doyle MD, PhD for their review of the manuscript and comments. This work was supported by the following grants ONR N0014-91-C-0134, DOE DE-FG03-91ER61227 and NIH 5P41RR01192. Dr Wong is supported by the Research Fund of the American Otological Society.

REFERENCES

1 Perkins RC. Laser stapedotomy for otosclerosis. *Laryngoscope* 1980, **90**:228–41
2 Schindler RA, Lanser MJ. The surgical management of cholesteatoma—the contribution of the laser. In: Tos M, Thomsen J, Peitersen E (eds) Third International Conference on Cholesteatoma and Mastoid Surgery, Copenhagen, Denmark June 5–9, 1988:769–78
3 Thedinger BS. Applications of the KTP laser in chronic ear surgery. *Am J Otol* 1990, **11(2)**:79–84
4 McGee TM. The argon laser in surgery for chronic ear disease and otosclerosis. *Laryngoscope* 1983, **93**:1177–82
5 Bartels LJ. KTP laser stapedotomy: Is it safe? *Otolaryngol Head Neck Surg* 1990, **103(5)**:685–92
6 Gherini S, Horn KL, Causse J-B, McArthur GR. Fiberoptic argon laser stapedotomy: Is it safe? *Am J Otol* 1993, **14(3)**:283–9
7 Hodgson RS, Wilson DF. Argon laser stapedotomy. *Laryngoscope* 1991, **101**:230–3

8 Lesinski SG, Stein JA. CO_2 laser stapedotomy. *Laryngoscope* 1989, **99**:20–4
9 Wiet RJ, Causse J-B, Shambaugh JGE, Causse JR. *Otosclerosis (Otospongiosis).* Alexandria, VA: American Academy of Otolaryngology—Head and Neck Surgery Foundation Inc, 1991
10 Gantz B. Argon laser stapedotomy. *Ann Otolaryngol* 1982, **91**:25–6
11 Jovanovic S, Schonfeld U, Berghaus A et al. CO_2 laser in stapes surgery. Proceedings *SPIE* 1993, **1876**:17–27
12 Kautzky M, Trodhan A, Susani M, Schenk P. Infrared laser stapedotomy. *Eur Arch Oto rhino laryngol* 1991, **248(8)**:449–51
13 Shah UK, Poe DS, Rebeiz EE et al. Erbium laser in middle ear surgery: In vitro and in vivo animal study. Proceedings *SPIE* 1994, **2128**:12–16
14 Stubig IM, Reder PA, Facer GW et al. Holmium-Yag laser stapedotomy: Preliminary evaluation. Proceedings *SPIE* 1993, **1876**:10–16
15 Segas J, Georgiadis A, Christodoulou P et al. Use of the excimer laser in stapes surgery and ossiculoplasty of middle ear ossicles: Preliminary report of an experimental approach. *Laryngoscope* 1991, **101**:186–91
16 Wong BJF, Dickinson MR, Neev J et al. Surface characteristics of argon laser ablated bone in the presence and absence of an initiator. *SPIE Proceedings* 1995, **2391**:366–78
17 Foth H-J, Barton T, Horman K et al. Possibilities and problems of using the holmium-laser in ENT. Biomedical Optics 1994 (technical abstracts) Society of Photo-Optical Instrumentation Engineers, Los Angeles, 1994: **2128**:21
18 April MM, Rebeiz EE, Aretz HT, Shapshay SM. Endoscopic holmium-laser laryngotracheoplasty in animal models. *Ann Otolrhino laryngol* 1991, **100**:503–7
19 Shapshay SM, Rebeiz EE, Bohigian K et al. Holmium-Yttrium aluminum garnet laser-assisted endoscopic sinus surgery: Laboratory experience. *Laryngoscope* 1991, **101**:142–9
20 Kautzky M, Susani M, Steurer M, Hofler H. Holmium-YAG-laserchirurgie eines nasopharynxkarzinoms. *Laryngo rhino otologie* 1993, **72**:181–6
21 Dillingham MF, Price JM, Fanton GS. Holmium laser surgery. *Orthopedics* 1993, **16(5)**:563–6
22 Nelson JS, Orenstein A, Liaw L-HL, Berns MW. Mid-infrared erbium-YAG laser ablation of bone: The effect of laser osteotomy on bone healing. *Lasers Surg Med* 1989, **9**:362–74
23 Nelson JS, Yow L, Liaw L-H et al. Ablation of bone and methacrylate by a prototype mid-infrared erbium-YAG Laser. *Lasers Surg Med* 1988, **8**:494–500
24 Nuss RC, Fabian RL, Sarkar R, Puliafito CA. Infrared laser bone ablation. *Lasers Surg Med* 1988, **8**:381–91
25 Walsh Jr JT, Flotte TJ, Deutsch TF. Er-YAG laser ablation of tissue: Effect of pulse duration and tissue type on thermal damage. *Lasers Surg Med* 1989, **9**:314–26
26 Walsh Jr JT, Deutsch TF. Er-YAG laser ablation of tissue: Measurement of ablation rates. *Lasers Surg Med* 1989, **9**:327–37
27 Li Z-Z, Reinisch L, Van de Merwe WP. Bone ablation with Er-YAG and CO_2 laser: Study of thermal and acoustic effects. *Lasers Surg Med* 1992, **12**:79–85
28 Stein E, Sedlacek T, Fabian RL, Nishioka NS. Acute and chronic effects of bone ablation with a pulsed holmium laser. *Lasers Surg Med* 1990, **10**:384–8
29 Wong BJF, Liaw L-HL, Neev J, Berns MW. Scanning electron microscopy of otic capsule and calvarial bone ablated by a holmium-YAG laser. *Lasers Med Sci* 1994, **9**:249–60

Key words: Bone histology; Holmium-YAG laser; Infra-red lasers; Laser surgery; Photo ablation; Otology; Stapes; Otosclerosis